International Journal of Heat and Mass Transfer 55 (2012) 1375–1384

Contents lists available at SciVerse ScienceDirect

International Journal of Heat and Mass Transfer

journal homepage: www.elsevier.com/locate/ijhmt

Prediction of fully developed turbulent heat transfer of internal helically ribbed tubes – An extension of Gnielinski equation

Wen-Tao Ji, Ding-Cai Zhang, Ya-Ling He, Wen-Quan Tao *

Key Laboratory of Thermo-Fluid Science and Engineering of MOE, School of Energy and Power Engineering, Xi'an Jiaotong University, Xi'an 710049, PR China

ARTICLE INFO

Article history:
Received 29 June 2011
Received in revised form 20 August 2011
Accepted 20 August 2011
Available online 8 November 2011

Keywords:
Heat transfer
Rib
Friction factor

ABSTRACT

Turbulent heat transfer and friction factors are measured in this paper for 16 internally grooved tubes with different geometrical parameters. Experiments are conducted for the 16 tubes with the Reynolds number range from 10,000 to 100,000 and Prandtl number from 4.98 to 8.22. Other parameter ranges are: $1 \leqslant N_s \leqslant 45$, $0.016 \leqslant e/d_i \leqslant 0.04$, $13 \leqslant \alpha \leqslant 45$, where N_s is the number of circumferential micro-fins (number of starts), e and α are the height and helix angle of the micro-fin, respectively, and d_i is the inner diameter of the embryo tube. An equation for predicting the average heat transfer of the inner helically ribbed tubes is presented based on Gnielinski equation with the friction factor in the numerator of the original Gnielinski equation being replaced by the measured friction factor in the fully developed flow region of the internally grooved tubes. For all data of the 16 tubes, most of the relative deviation is within ±10%. Comparison of this equation with other data available in the literature is also provided, and the deviation of more than 93% of the compared data is within ±20%, 99% within ±40%. Since the friction factor is easier to be measured, the proposed correlation equation is practically very applicable and its accuracy is also acceptable for the engineering design.

1. Introduction

Gnielinski equation [1] is the comparably most accurate formulation in predicting the average turbulent convection heat transfer of smooth tubes and channels and widely adopted nowadays in heat transfer calculations [2–5]. Based on analysis on a large number of data from very wide literature sources, the proposed equation can predicts nearly 90% of about 800 experimental results within deviations of ±20%. The correlation is as follows:

$$\mathrm{Nu} = \frac{(f/8)(\mathrm{Re}-1000)\mathrm{Pr}}{1+12.7(f/8)^{1/2}(\mathrm{Pr}^{2/3}-1)}\left[1+\left(\frac{d_i}{L}\right)^{2/3}\right]\left(\frac{\mathrm{Pr}}{\mathrm{Pr_w}}\right)^{0.11}, \quad (1)$$

where the friction factor f is calculated from the equation of Filonenko [6]:

$$f = (1.821\ \mathrm{gRe} - 1.64)^{-2}. \quad (2)$$

The application range of Eq. (1) is: $\mathrm{Re} = 2300 - 10^6$, $\mathrm{Pr} = 0.6 - 10^5$. In the transition region of $2300 < \mathrm{Re} < 10^4$, the equation can also satisfactorily predicts the heat transfer coefficient.

Apart from its accuracy, wide application range is the most important feature of Eq. (1) which couples heat transfer coefficient and friction factor compared with most of other experimental correlations. Historically, correlating heat transfer with friction factor in the prediction of turbulent heat transfer was originally from the theory of analogy between turbulent flow and convective heat transfer. The so-called Reynolds analogy, Prandtl analogy and von Karmann analogy are the major outcomes of such analogy theory. Prandtl proposed following correlation for fully developed turbulent heat transfer in tubes in 1944 [7]:

$$\frac{\mathrm{Nu}}{\mathrm{RePr}} = \frac{f/8}{1+8.7(f/8)^{1/2}(\mathrm{Pr}-1)}. \quad (3)$$

From 1950 to 1970, there were many published experimental and analytical results about the turbulent heat transfer and friction in tubes and channels, among which the work of Petukhov et al. is the most important [8,9]. Based on the integration of the governing equation of turbulent heat transfer in tubes with some simplified treatment Petukhov provided [9] a simplistic relationship form of heat transfer prediction correlation for fully developed turbulent flow as follows:

$$\frac{\mathrm{Nu}}{\mathrm{RePr}} = \frac{f/8}{1.07+12.7(f/8)^{1/2}(\mathrm{Pr}^{2/3}-1)}, \quad (4)$$

where the friction factor f is calculated from the equation of Filonenko as shown above.

According to Petukhov's research, this equation can predict experimental results with an accuracy of 5–6% over a range of Reynolds number from 10^4 to 5×10^6 and Pr number from 0.5 to

* Corresponding author.
E-mail address: wqtao@mail.xjtu.edu.cn (W.-Q. Tao).

0017-9310/$ - see front matter © 2011 Elsevier Ltd. All rights reserved.
doi:10.1016/j.ijheatmasstransfer.2011.08.028

Nomenclature

A	area (m^2)
c_p	specific heat capacity ($J\,kg^{-1}\,K^{-1}$)
d	diameter of tube (mm)
e	height of internal micro-fin (mm)
f	friction factors (dimensionless)
h	heat transfer coefficients ($W\,m^{-2}\,K^{-1}$)
N_s	number of starts
L	tested length of tube (m)
m	mass flow rate ($kg\,s^{-1}$)
Nu	Nusselt number (dimensionless)
Pr	Prandtl number
p	axial rib pitch (mm)
q	heat flux ($W\,m^{-2}$)
Re	Reynolds number
R_w, R_f	thermal resistance of tube wall and fouling layer ($m^2\,kW^{-1}$)
T	temperature (°C)
t_b	fin thickness at base (mm)
t_t	fin thickness at tip (mm)

Greek symbols

φ	heat transfer rate (W)
λ	thermal conductivity ($W\,m^{-1}\,K^{-1}$)
ΔT_m	logarithmic mean temperature difference (K)
α	helix angle (deg)
η	efficiency index (dimensionless)

Subscript

c	condensing
e	evaporating
i	inside of tube
o	outside of tube
p	plain surface
r	internal ribbed tube
s	saturation
w	wall

200. For the Prandtl number range from 0.5 to 2000, the accuracy reduced to 10% at the same range of Re.

However, it can be observed that the above mentioned correlations are all used to calculate the convection heat transfer of smooth tubes or channels with a certain micro-roughness generally from 0.3 to 0.4 μm. In recent years, with the further development of enhanced surfaces outside tube for boiling and condensation in refrigeration engineering, the outside tube thermal resistance becomes smaller and smaller, making the tube-side enhancement important. After the patent release of internal helically-ribbed tubes in 1977 [10], this kind of enhanced tubes have been ever-increasingly adopted in many engineering applications, because it can provide significant heat transfer enhancement ratio compared with smooth tubes. Especially in the refrigeration engineering, this is proved to be an efficient enhanced technique in conjunction with enhancing techniques on outside surface. The so-called doubly-enhanced tubes are the outcome of such application. In the large shell and tube heat exchangers of building air conditioning, the water flows through the inner side of helically ribbed tubes and refrigerant is boiling or condensing outside. As shown by Fig. 1, these tubes can provide the water-side enhancement up to 250% of the smooth tube according to [11]. Our experimental measurements also show high enhancement effect which will be shown later.

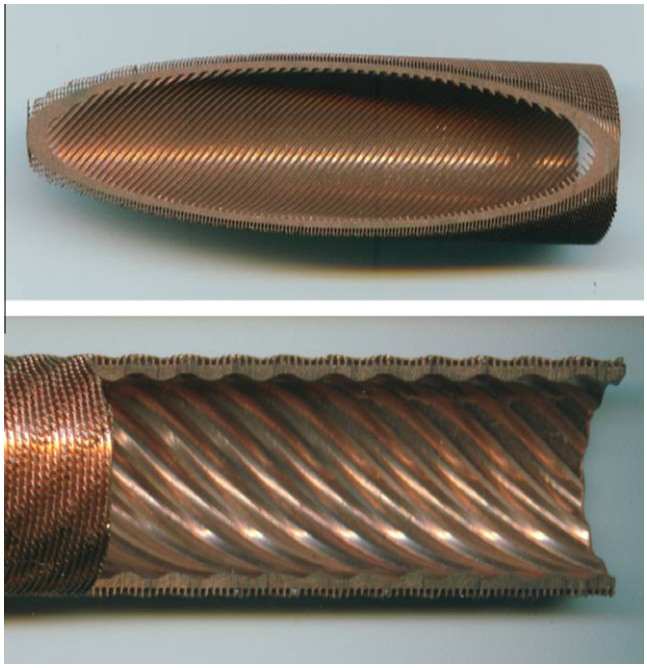

Fig. 1. Photos of internal grooved tubes.

For the heat exchanger design with doubly enhanced tubes, accurate predictions of both inside and outside heat transfer coefficients are of equal importance because in such cases the inside and outside thermal resistances are comparable. In literatures there are a large number of test results for the tube outside boiling or condensation. However, the information of tube inner side heat transfer coefficient of helically ribbed tubes is very scarce. Following is a brief review on this regard.

First, the measurement method is concerned. Because of the complexity of the surface structure it is very difficult, if not impossible, to directly measure the helically-ribbed tube wall temperatures to determine the heat transfer coefficient of the inner enhanced tubes. Wilson Plot is almost the only choice adopted in the literatures [12–18].

For the heat transfer study of helically enhanced tubes, Ravigururajan and Bergles [19] gathered a wide range of tube parameters from 17 research papers with tube geometry of e/d: 0.01–0.2; p/d: 0.1–7.0; α/90: 0.3–1.0; flow parameters Re: 5000–250,000 and Pr: 0.66–37.6. Based on the rib profiles and flow parameters, general correlations of pressure drop and heat transfer were developed as follows:

$$\text{Heat transfer correlation}: \mathrm{Nu}_r/\mathrm{Nu}_p = \{1 + [2.64\mathrm{Re}^{0.036}(e/d)^{0.212} \times (p/d)^{-0.21}(\alpha/90)^{0.29}(\mathrm{Pr})^{0.024}]^7\}^{1/7}. \tag{5a}$$

$$\text{Friction factor}: F_r/f_p = 0.25 \times \left\{1 + \left[29.1\mathrm{Re}^{(0.67-0.06p/d-0.49\alpha/90)} \times (e/d)^{(1.37-0.157p/d)} \times (p/d)^{(-1.66\mathrm{Re}\times 10^{-6}-0.15p/d)} \times (1 + 2.94\sin(45/Ns))\right]^{15/16}\right\}^{16/15}. \tag{5b}$$

In the two correlations, Nu_p and f_p are calculated from the equations of Petukhov and Filonenko as shown in Eqs. (4) and (2).

It was claimed in [19] that Eq. (5b) can predict 96% of the database (1658 points) within deviations of ±50% and 77% within ±20%, and for Eq. (5a), the prediction results for heat transfer of 18070 points are 99% within deviations of ±50% and 69% within ±20%. In the subsequent research of Webb et al. [20], it is shown that the correlations of Ravigururajan and Bergles [19] over predicts the heat transfer coefficient of 7 tubes by 10–45%, and the predicted friction data had an error of ±30%.

Webb et al. [20] also presented experimental data fitted equations for heat transfer coefficients and friction factor of internal helically-enhanced tubes, with number of starts, rib height and helix angle as parameters:

$$\text{Heat transfer}: j = StPr^2/3\nabla 0.00933\mathrm{Re}^{-0.181}N_s^{0.285}\sum(e/d_i)^{0.323}\alpha^{0.50} \tag{6a}$$

$$\text{Friction factor}: f = 0.108\mathrm{Re}^{-0.283}N_s^{0.221}(e/d_i)^{10.785}\prod^{0.785}\alpha^{0.78} \tag{6b}$$

($0.024 \leqslant e/d_i \leqslant 0.041$, $2.39 \leqslant p_e/e \leqslant 12.84$, $25 \leqslant \alpha \leqslant 45°$, $\beta = 41$, $t_t/d_i = 0.015$).

The average deviations of the predicted friction and heat transfer results from experimental data are respectively of 2.9% and 3.8% for the 7 tubes of their experiments.

From the correlations provide above, it can be observed that all the proposed correlations include the characteristic parameters of the inner enhanced tubes: number of starts, rib height and helix angle. From academic point of view including these rib geometric parameters in the prediction equations are reasonable which can be obtained by special industrial microscopic instrument; however, this practice provides some inconvenience to the engineering applications of the proposed correlations.

Numerical simulations are widely adopted to predict the turbulent fluid flow and heat transfer characteristics of different channels, and many computational models and methods are proposed. Home et al. [21] numerically investigated the fully developed turbulent fluid flow in a square duct by the detached eddy simulation based (DES) turbulence model (Strelets version, [22]). Assato and de Lemos [23] used the linear and nonlinear eddy-viscosity models to predict the turbulent flow of periodically sinusoidal-wave channels. As far as the fully developed turbulent flow and heat transfer in internally enhanced channels are concerned, only limited references recently published are known to the present authors. Liu and Jensen [24] numerically studied the effect of rectangular, triangular and round-crest fins on the Nusselt number and friction factors of the internally grooved tubes. The high Reynolds number $k-\varepsilon$ turbulence model was applied to the fully turbulent central region and a one-equation turbulence model (Norris and Reynolds version, [25]) is applied to the near-wall fin region. For tubes with number of starts equal to or more than 14 their numerical results show that the efficiency index, i.e., $(\mathrm{Nu}/\mathrm{Nu}_p)/(f/f_p)$, for three types of fins are larger than 0.8. Norris Iii [25] recently made an in-depth numerical analysis for the fully developed turbulent flow and heat transfer of internally finned tubes. The fin parameters of their study included the number of fins ($8 \leqslant N_s \leqslant 54$), none dimensional fin height ($8 \leqslant 2e/d_i \leqslant 54$) and fin width ($0.024 \leqslant 0.5(t_b + t_t)/d_i \leqslant 0.042$), and helix angle ($30° \leqslant \alpha \leqslant 45°$). Different $k-\varepsilon$ and $k-\omega$ turbulence models were implemented and evaluated. It was found that laminarization in the interfin region plays an important role, particularly at low Reynolds numbers. For the computer aided simulation, the accuracy and stability of the solution are heavily affected by the turbulence model adopted. Thus it is highly required that some experimental correlations to be developed which can be used to verify, at least partially, the reliability of simulation results.

In this paper, the authors seek for another way by the simulation of heat transfer analogy briefly presented above. For the convenience of engineering application, it is highly desired that if we could correlate the friction factor of the enhanced tube in the fully developed region which is easy to be measured to the heat transfer characteristics just as the analogy theory between Nu and f for the smooth tube. By carefully analyze the experimental results presented in literatures, we have found that the efficiency index, $\eta = (h/h_p)/(f/f_p)$, of many researches on inner enhanced tubes generally fluctuates around 1 ± 0.2 with fluid of water [11,20,27]. Here, h and h_p are, respectively, the heat transfer coefficient of enhanced tubes obtained by experiments and the heat transfer coefficient of plain tube calculated by Gnielinski equation, Eq. (1), f and f_p are the friction factor of enhanced tube determined by test and that of plain tube calculated by Eq. (2). Table 1 gives a summary of the tested cases in [11,20,27], where d_i is the inner diameter of the original embryo tube.

Table 1
Summary of geometry parameters and heat transfer performances of helically grooved tubes in [20] (Re = 27,000, Pr = 5.2), [11] (d_o = 19.05 mm, Re = 25,000, Pr = 10.4),and [26] (d_o = 19.05 mm, Re = 27,000, Pr = 9.35).

Tube	d_i(mm)	e(mm)	N_s	α(deg)	p/e	h/h_p	f/f_p	η
Tube 1 [20]	15.54	0.327	45	45	2.81	2.32	2.74	1.18
Tube 2 [20]	15.54	0.398	30	45	3.50	2.33	2.45	1.05
Tube 3 [20]	15.54	0.430	10	45	9.88	1.74	1.65	0.95
Tube 4 [20]	15.54	0.466	40	35	3.31	2.26	2.35	1.04
Tube 5 [20]	15.54	0.493	25	35	5.02	2.08	2.10	1.01
Tube 6 [20]	15.54	0.532	25	25	7.05	1.93	2.03	1.05
Tube 7 [20]	15.54	0.554	18	25	9.77	1.51	1.48	0.98
GEWA-TW™ [11]	15.3	0.245	1	89	5.3	1.40	1.40	1.00
Thermoexcel-CC™ [11]	14.97	0.374	1	73	46.7	1.59	1.90	0.84
GEWA-SC™ [11]	15.02	0.526	25	30	2.67	1.87	1.65	1.13
Korodense™ (LPD) [11]	17.63	0.705	1	81	20.3	1.89	2.26	0.84
Turbo-Chil [11]	14.60	0.380	10	47	11.1	1.98	1.83	1.08
Korodense™ (MHT) [11]	17.63	0.441	1	81	12.0	2.5	4.63	0.54(?)
Tred-26d™ [11]	14.45	0.347	10	45	7.63	2.24	1.88	1.19
Turbo-B™ [11]	16.05	0.449	30	35	1.94	2.34	2.14	1.09
Turbo-BIII LPD [11]	16.38	0.360	34	49	3.56	2.40	1.98	1.21
Turbo-BIII [11]	16.38	0.410	34	49	3.22	2.54	2.30	1.10
Tred-19d™ [11]	14.45	0.347	10	57	7.63	2.55	1.76	1.45(?)
A8 (Table 9.8) [11]	13.5	0.486	2	57	7.6	3.75	3.35	1.11
AC1 [26]	17.59	0.51	–	–	6.08	2.97	2.78	1.07
AC2 [26]	17.27	0.38	–	–	8.16	2.77	2.66	1.04
AC3 [26]	17.32	0.43	–	–	3.95	3.72	4.38	0.85

Webb et al. indicated in [28] that for the tube with repeated-rib roughness the friction factor data can be well correlated by using law of the wall similarity. And based on the wall similarity the heat-momentum transfer analogy can adequately correlate the repeated-rib heat transfer data.

From the existing experimental results and the idea of analogy between turbulent heat transfer and friction, it is reasonably to assume that the efficiency index takes a value of 1, and then we have

$$h = h_p \frac{f}{f_p}, \tag{7}$$

where f_p, h_p are friction factor and heat transfer coefficient of smooth tube predicted by Filonenko equation and Gnielinski equation, respectively. From Eq. (7) we get following extended Gnielinski equation for prediction of heat transfer of internal helically-ribbed tubes:

$$\mathrm{Nu} = \frac{(f/8)(\mathrm{Re}-1000)\mathrm{Pr}}{1+12.7(f\mathrm{p}/8)^{1/2}(\mathrm{Pr}^{2/3}-1)}\left[1+\left(\frac{d_i}{L}\right)^{2/3}\right]\left(\frac{\mathrm{Pr}}{\mathrm{Pr}_w}\right)^{0.11}. \tag{8}$$

In this paper, heat transfer and friction characteristics of 16 different inner grooved tubes are measured for water, then verification of this extended Gnielinski equation is conducted with the experimental results. The prediction results of Eq. (8) is also compared with experimental results or fitted equations of related publications in the recent years.

In the following, the test apparatus is first described, followed by test procedure and data reduction method. Then the verification and comparisons will be conducted. Finally some conclusion will be drawn.

2. Experimental apparatus

The experimental apparatus consists of a measurement system and three circulatory systems: refrigerants and two water circulating systems. In experiment, water is flowing inside and refrigerant R134a is condensing or boiling outside of the inner helix-grooved tubes. A schematic figure of the test apparatus is shown in Fig. 2.

The refrigerant circulating system includes the boiler vessel, condenser vessel, and two ducts connecting the two vessels, which are all made of stainless steel. The inner diameter of boiler is 257 mm, with length of 1100 mm; the inner diameter of condenser is 147 mm, with length of 1500 mm. The whole apparatus is well insulated with insulating rubber plastic material of thickness 40 mm and one layer of aluminum foil is used to enwrap the rubber plastic outside. In experiment, the heating water is flowing through the inner side of the test tube, which is placed in the boiling or condensing vessel, and then going through the weight-time flow meter before it returns to the water tank via a centrifugal pump.

When testing the heat transfer characteristics of the condenser, the cooling water flows through the inner side of helically-ribbed tubes, refrigerants is condensing outside of the surface, and the refrigerant vapor is converting to liquid and gets back to the boiler through the duct between the boiler and condenser. The water flowing through the tubes in the boiler provides heat to produce vapor for the condenser. The saturated temperatures of the condenser and boiler are maintained constant by adjusting the flow rate and inlet temperature.

The test procedure for the characteristics of the evaporator is similar. The difference is only in the measurement purpose.

A pressure gauge is used to measure the pressure of the boiler vessel. The range of the measurement is 0–2.5 MPa and the precision is 0.25%. The temperatures of the refrigerant in different part of the system are measured by platinum resistance temperature transducers (PT100) which have a precision of ±(0.15 + 0.002|t|)K at the test range. The difference between inlet and outlet water's temperature of heating and cooling is measured by a six-junction copper-constantan thermocouple pile. Thermocouples are used to measure the temperatures of inlet and outlet of heating and cooling water. The thermocouples and thermocouple piles were calibrated against a temperature calibrator that had the precision of 0.2 K. A capacitive differential pressure transmitter with class of precision ±0.2% and measurement range of 0–37.4 kPa was used to measure the pressure drop. A Keithley digital voltmeter having the resolution of 0.1 V is used to measure the electric potential of the thermocouples and thermocouple piles.

The average heat flux and refrigerant saturated temperature are held constant during each test run.

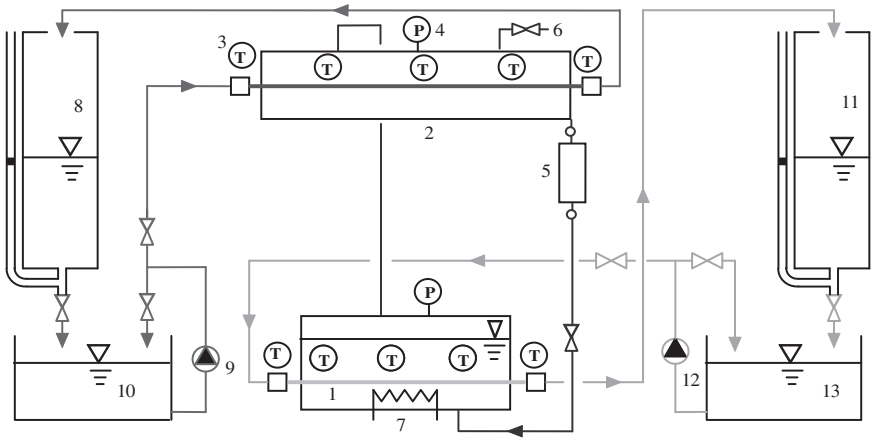

(1)Boiler;(2)condenser;(3)thermocouple;(4)pressure gauge;(5) condensate measuring container;(6)exhausting valve;(7)subsidiary electric heater;(8)weight-time flow meter of cooling water;(9)cooling water pump;(10)cold water storage tank; (11) weight-time flow meter of hot water; (12)hot water pump; (13)hot water storage tank.

Fig. 2. Schematic diagram of the experimental apparatus.

Table 2
Specifications of Nos. 1–11.

Tube code	Outside diameter d_o(mm)	Inside diameter d_i(mm)	Height of inside fin e(mm)	Number of starts N_s	Helix angle α(deg)	Fin thickness at base t_b(mm)	Fin thick-ness at tip t_t(mm)	Length of test section L(mm)
Plain	19.09	16.41						1100
No. 1	19.00	16.63	0.338	45	30	0.821	0.507	1331
No. 2	19.1	16.49	0.293	43	30	0.743	0.451	1310
No. 3	18.92	16.66	0.351	38	30	0.826	0.287	1330
No. 4	18.97	16.63	0.374	45	25	0.914	0.457	1330
No. 5	19.07	16.59	0.357	43	18	0.765	0.306	1333
No. 6	19.10	16.66	0.334	45	20	0.668	0.292	1325
No. 7	19.00	16.55	0.331	45	35	0.534	0.267	1300
No. 8	18.90	16.66	0.456	13	35	3.00	1.320	1490
No. 9	18.92	16.70	0.340	45	27	0.680	0.340	1500
No. 10	19.04	16.66	0.361	43	22	0.552	0.276	1090
No. 11	18.99	16.61	0.346	45	40	0.622	0.216	1095

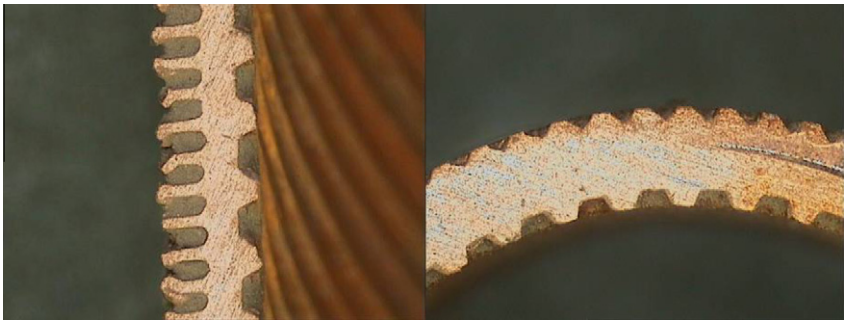

Fig. 3. One of the enhanced tubes' cross section.

The specifications of the test tubes (Nos. 1–11) are given in Table 2. An example of the enhanced tubes' cross section is given in Fig. 3(a). The specifications of tested tube geometries include the embryo tube's outside diameter, inner fin height (e), number of starts (N_s), helix angle (α), fin base thickness (t_b), fin tip thickness t_t and the length of test section (L), as shown in Fig. 3(b).

To insure that the heat transfer coefficient was not influenced by the entrance effect, there is an average length of 320 mm before the test section. In this study, the tubes of Nos. 1–11 are tested for condensing, and Nos. 12–16 are tested for boiling heat transfer.

3. Experimental procedures

After the start of the test apparatus, the major operation parameters (water flow rates, temperature difference of water and the saturated temperature) are regulated so that the desired test regime can be soon reached. The working medium is refrigerant R134a and its condensing and boiling temperatures are maintained at 40 °C and 10 °C, respectively. During a data run, the average heat flux and saturated temperature were all held constant. It should be noted that since the natural circulation of the refrigerant is adopted in our test apparatus, both condenser and evaporator are at the same saturated temperature. That means when the system is working on the condensing regime, the boiling temperature is also 40 °C, while for boiling regime the condensation temperature is maintained at 10 °C.

After the system was in the steady state the test data were taken. The steady state was characterized by (1) the variation of the required saturation temperature of refrigerant was in the allowed range, usually ±0.02 K of Keithley-monitored result, and (2) the fluctuation of water temperature at inlet and outlet of the condenser and boiler was within ±0.1 K, mostly within ±0.05 K.

In the experiment, the water Re number spans from 10,000 to 100,000. For each tested tube, generally 6–9 flow rates were measured.

4. Data reduction and uncertainty analysis

From measured quantities, the following energy balance is first examined.

Heating power input from heating water:

$$\phi_e = m_e c_p (t_{e,1} - t_{e,2}) \tag{9}$$

Cooling power output from cooling water:

$$\phi_c = m_c c_p (t_{c,2} - t_{c,1}). \tag{10}$$

In the two equations, $t_{e,1}$, $t_{e,2}$ are the inlet and outlet temperatures of heating water (K), $t_{c,1}$, $t_{c,2}$ are the inlet and outlet temperatures of cooling water (K), c_p is the specific heat capacity of water corresponding to the mean temperature of inlet and outlet water (J/kg K), $\dot{m}_e$, $\dot{m}_c$ are the mass flow rates of heating water and cooling water (kg/s). The properties of water are taken from [5].

The allowed maximum difference between these two heat transfer rates was within 3%. And the mean value of the two heat transfer rates, Φ, was used to determine the overall heat transfer coefficient of the test tube.

The overall heat transfer coefficient is determined by the following equation.

$$k = \frac{\phi}{Ao \cdot \Delta tm} \tag{11}$$

The outside surface area A_o is calculated as follows:

$$A_o = \pi d_o L \tag{12}$$

where d_o is the outside diameter of the embryo test tube, from which the integral-fin tube and enhanced surface was manufactured. L is the length of tube's test section.

The average temperature difference between the saturated temperature of refrigerant and fluid, Δtm, is the log-mean temperature difference, which is defined as follows:

$$\Delta t_m = \frac{|t_{w,in} - t_{w,out}|}{\ln\left(\frac{t_s - t_{w,out}}{t_s - t_{w,in}}\right)}. \quad (13)$$

In this equation, t_s is the saturation temperature of refrigerant in the pool of the boiler, $t_{w,in}$ is the temperature of the inlet water and $t_{w,out}$ is the temperature of the outlet water.

In order to obtain the water side heat transfer coefficients of different enhanced tubes, the thermal resistance separation method, i.e., Wilson plot technique was adopted.

This method requires that the phase change side heat transfer coefficient held to be constant when separating the waterside thermal resistance from the overall heat transfer resistance. The overall thermal resistance $1/k$ can be separated into four parts:

$$\frac{1}{k} = \frac{A_o}{A_i}\frac{1}{h_i} + R_w + \frac{1}{h_o} + R_f, \quad (14)$$

where R_f is the fouling thermal resistance. It was neglected in the present study for that at the beginning of experiment we had cleaned the inner and outer surface using acetone solution, the heating water used was neat enough and the running time of one tested tube was two days at most. R_w is the thermal resistance of the wall. A_o and A_i are the area of tested tube's outside and inside surfaces. h_o and h_i are the outside phase change heat transfer coefficient and inside water heat transfer coefficient, respectively. It should be noted that for the doubly-enhanced tube both the inside and outside heat transfer surfaces are determined by the diameters of its embryo tube.

To proceed, the saturated temperature of refrigerant and the heat flux should be kept constant to ensure that h_o is maintained unchanged during the test. For a given tube geometry, assuming that the heat transfer coefficient of the enhanced inner surface can be represented by $c_i h_{ip}$, where h_{ip} is the heat transfer coefficient determined by Gnielinski equation at the same fluid velocity and reference temperature. Then Eq. (14) can be changed into:

$$\frac{1}{k} = a\frac{1}{h_{ip}} + b, \quad (15)$$

where

$$a = \frac{d_o}{d_i}\frac{1}{c_i}, \quad (16)$$

$$b = \frac{1}{h_o} + R_w. \quad (17)$$

A group of the data is taken by varying the in-tube water velocity, and these data are expressed via the equation of a linear straight line shown by Eq. (15). By using data regression method the slope a and the constant term b of the linear straight line can be determined, hence the enhancement coefficient of c_i, water side and phase change side heat transfer coefficient can be determined respectively. It is worth noting that in the determining the water velocity of the inner tube the cross section area of $\pi d_i^2/4$ is used for both plain and helically-ribbed tube.

An uncertainty analysis according to literature [30,31] has been employed to estimate the possible uncertainty of experimental data and the reduced results. The confidence level for all measurement uncertainties are 95% except indicated individually. The estimated uncertainty of f is within 7.1%, heat flux q of the tubes is within 5.7%, and that of k is within 9.3%. The error in the Wilson plot is calculated to be within 5%. Then, the uncertainties in h_i is considered of 20% [1]. As h_o was not directly measured, the uncertainty of h_o was estimated using the method suggested in [31]. It is estimated to be within 31.7% for the 16 tubes.

5. Experimental results and discussion

5.1. Reliability validation of experimental apparatus

In order to test the reliability of experimental apparatus, the experimental result of friction factor is firstly compared with Filonenko equation [6]. Fig. 4 is the comparison result. Within the Re number range from 8000 to 90,000, the relative deviation of experiment data from Filonenko equation is within ±5%.

At the saturated temperature of 40 °C, the condensing heat transfer coefficient of plain tube, both inside and outside, obtained by the thermal resistance separation method is also compared with Nusselt analytical solution, with the inner water side heat transfer coefficient being calculated by Gnielinski equation. Fig. 5 is the comparison result. It can be observed that the deviation from the analytical solution is within −10%. The comparison results confirm the reliability of the experimental apparatus.

5.2. Experimental verification of the extension of Gnielinski equation

The Wilson plots of Eq. (15) for 5 tubes tested are shown in Fig. 6 as representatives, from which the enhancement coefficient

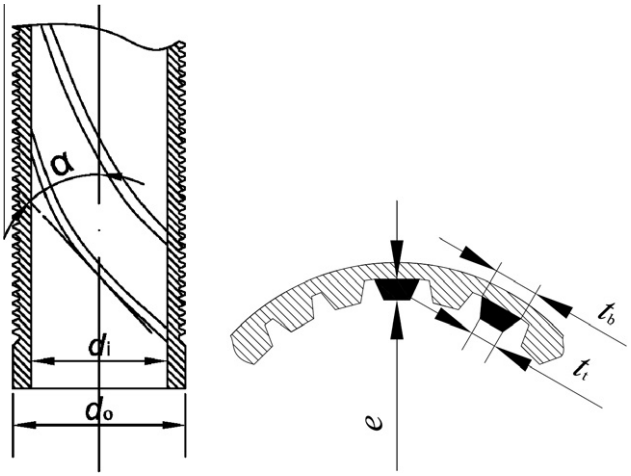

Fig. 4. The schematic diagram of tube cross section.

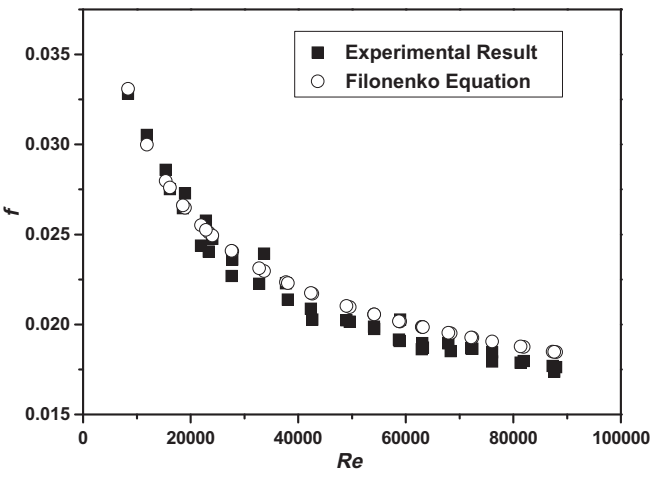

Fig. 5. Comparison of measured friction factor with Filonenko equation.

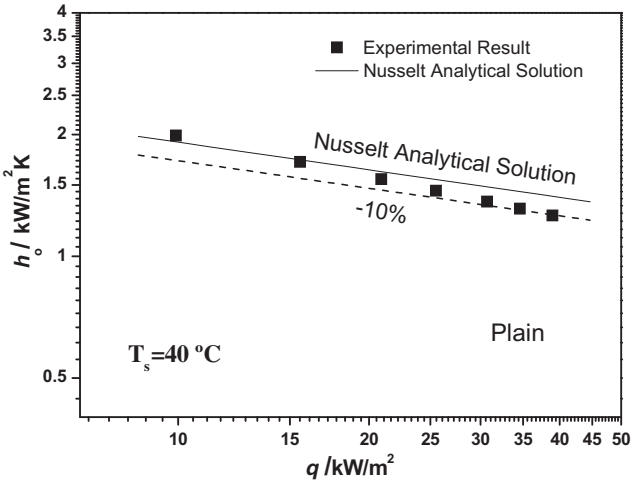

Fig. 6. Comparison of experimental result with Nusselt analytical solution.

Table 3
Water-side heat transfer enhanced coefficient of 16 tubes compared with plain tube.

Tube no.	No. 1	No. 2	No. 3	No. 4	No. 5	No. 6	No. 7	No. 8
c_i	2.61	2.51	2.54	2.71	2.36	2.48	2.79	2.06
Tube no.	No. 9	No. 10	No. 11	No. 12	No. 13	No. 14	No. 15	No. 16
c_i	2.44	2.57	2.94	2.39	2.83	2.72	2.60	1.71

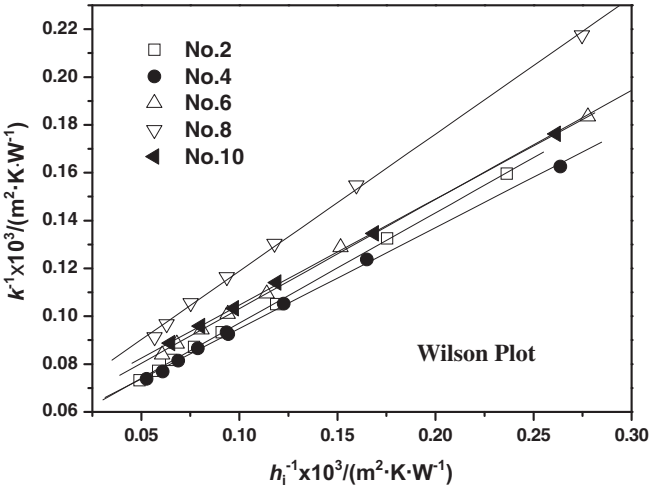

Fig. 7. Wilson plot of five tubes.

c_i in Eq. (16) can be obtained. The coefficients of all the test tubes are listed in Table 3. The enhanced ratio ranges from 1.71 to 2.94, depended on the different enhanced structures.

Come here we have two ways for the average inner heat transfer coefficient of the helically-ribbed tube: one is obtained by timing the heat transfer coefficient from Gnieleinki equation at the same water velocity by the enhancement coefficient c_i from the Wilson plot; The other is determined by the extended Gnielinski equation, Eq. (8), by using the Darcy friction factor determined by our experiments. The comparisons of these two results are shown in Figs. 7(a)–(p).

All the 152 data of water span Prandtl number from 4.98 to 8.22, and Reynolds number from 10,000 to 100,000. Generally speaking, the calculation results agree with the experimental results quite well. The largest relative deviation is −18.3% in tube No. 8. For all 16 tubes, 89% of the relative deviation is within ±10%. Fig. 8(a) and (b) are the relative deviation results of 16 tubes within the Re number tested.

6. Comparisons with other results

In the studies of Webb et al. [20], the inner helically ribbed tubes' heat transfer of water is presented. The enhanced ratio of these tubes spans from 1.51 to 2.32. Based on the friction curves fitted test data, Eq. (8) is used to predict Nusselt number. Fig. 9 compares their experimental results with Eq. (8) at Pr = 5.2, 20,000 ⩽ Re ⩽ 65,000. It can be observed that all the relative deviation of 7 tubes lies in the region of ±18%, and mostly within ±10%. In the figure, the tube's codes like 0.33/30/45 stand for the average height of rib in mm, the number of starts and the helix angle in degrees, respectively.

According to Webb et al. [20] comparison, the deviation of their correlation (Eqs. (6a) and (6b)) in predicting the heat transfer coefficient is within 10%, over predicting the friction factors 0–15%.

At the Prandtl number of 5.2, the prediction results of Eq. (8) are compared with the correlation of Webb in Fig. 10 for the tubes presented in the book of Webb and Kim [11]. The geometrical parameters is shown in Table 1, except the tube with starts N_s less than 10 (N_s = 10 was not excluded), as it does not meet the requirements of 25 ⩽ α ⩽ 45 of Eqs. (6a) and (6b). The friction factors of these tubes are predicted by Eq. (6b). With the range of Re from 10,000 to 100,000, Pr = 5.2, the deviation is within 5% and −15%. The largest deviation lies in the tubes with N_s of 10. Most of the deviation lies in the range of ±10%. It is also found that for the tube of Tred-19d^{TM}, the efficiency index in [11] is 1.45, while the deviation of calculation results of Eq. (8) from Eq. (6a) is from 0.85 to 0.9, in the range of ±20%.

In the experiment of Ravigururajan and Bergles [19], the correlations of Nu and f based on their data were developed. The experimental results of the four tubes tested in [19] are also compared with Eq. (8) in Fig. 11. We can observe that the deviations of all the data range from −40% to 20%, and 64% of experimental result is within ±20%. Ravigururajan and Bergles [19] indicated in their paper that their heat transfer correlation predicts 99% data to within ±50%. It seems that Eq. (8) can predict their test data with a less deviation than their correlation.

For three dimensional cone roughness in the research of Webb [27], the prediction errors of Eq. (8) is within ±20% of tube TC3. The comparison results of TC3 at Pr = 6.4 are shown in Fig. 12. From the efficiency index presented in Table 1, the prediction errors of TC1 and TC2 should also be within ±20%. Fig. 13

Totally 288 data are compared with Eq. (8), the deviation of 89% are within ±20%, 99% is within ±40%. It should be noted that the water Pr span in this experiment is seems to be a bit narrow in condition. Thus extension to a more wide water Pr should be careful and experimental verification is highly required.

7. Conclusions

The heat transfer of 16 internally grooved tubes are studied in this paper, an equation is proposed to predict the average heat transfer coefficient of the inner enhanced tubes. The following major conclusions can be drawn:

(1) From the literature review, the efficiency index is generally fluctuating in the range of 1 ± 0.2 for the internally grooved tubes' convective heat transfer of water. Thus, an equation based on Gnielinski equation is proposed and compared with experimental results of the 16 tubes. The proposed

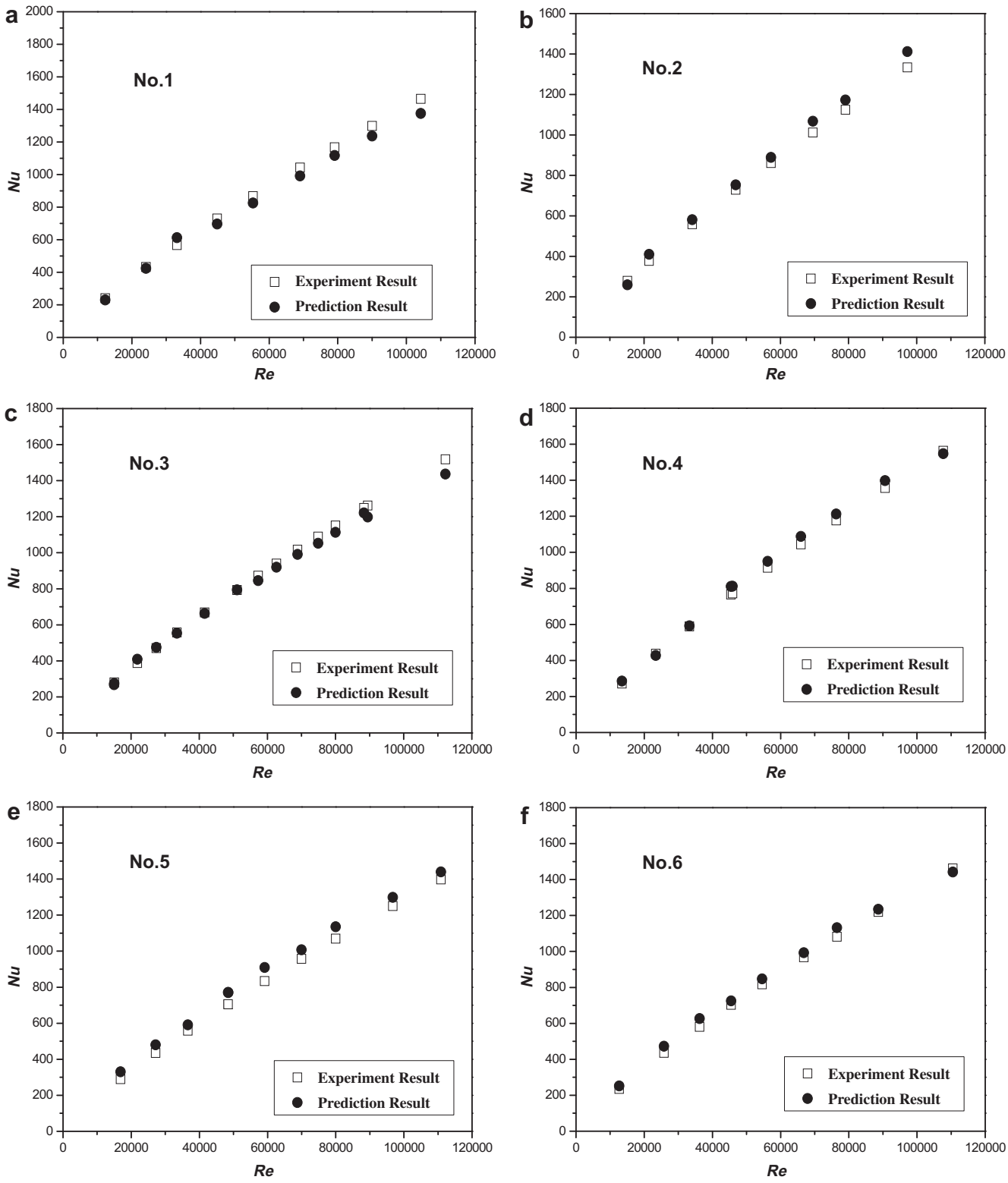

Fig. 8. Comparisons of experimental result with calculation result from extended Gnielinski equation.

equation can be regarded as the extension of the Gnielinski equation with the friction factor in its numerator being replaced by the friction factor in the fully developed flow region of the enhanced tube. Totally 440 data is compared, for 72% data the relative deviation is within ±10%, for 93% data deviation is within ±20%, and for more than 99% is within ±40%.

(2) Compared with the results of commercial internally grooved or three-dimensional cone roughness tubes available in the literature, most of the deviation is within ±20%.
(3) Since the friction factor is easier to be measured, the proposed correlation equation is practically very applicable and its accuracy is also acceptable for the engineering design.

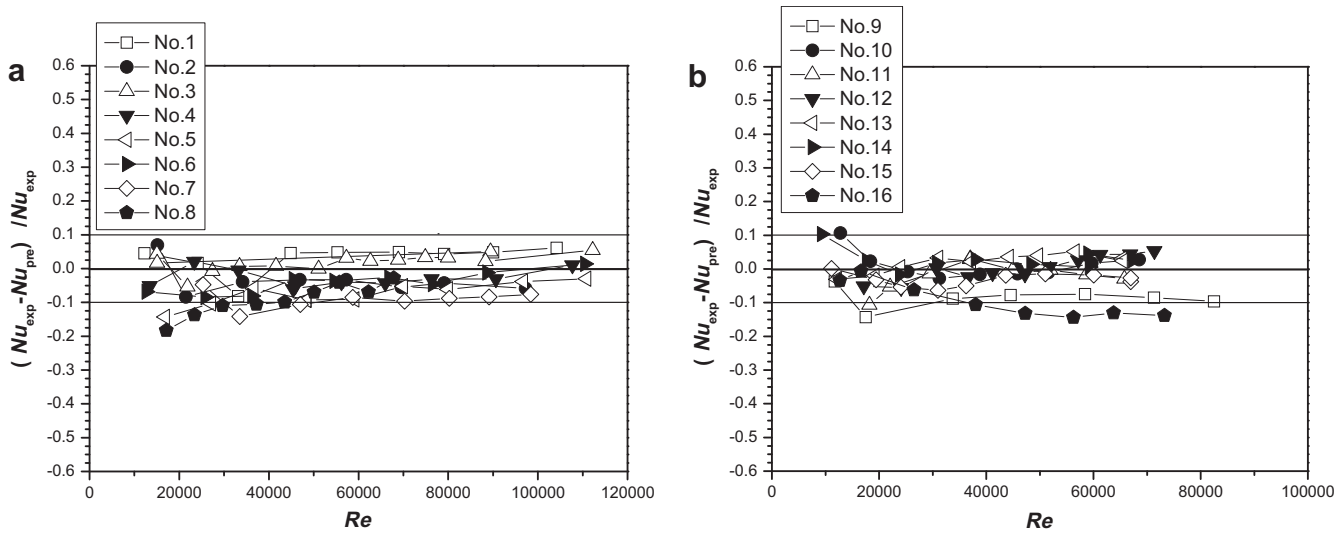

Fig. 9. Relative deviation of calculation result from experimental result.

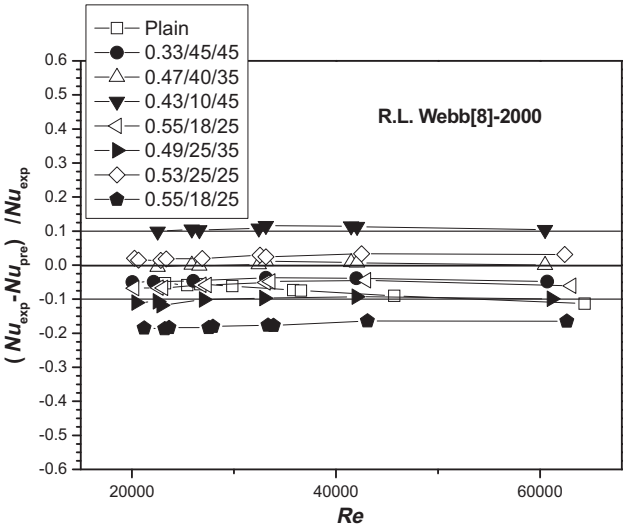

Fig. 10. Relative deviation of calculation result from experimental result in [20].

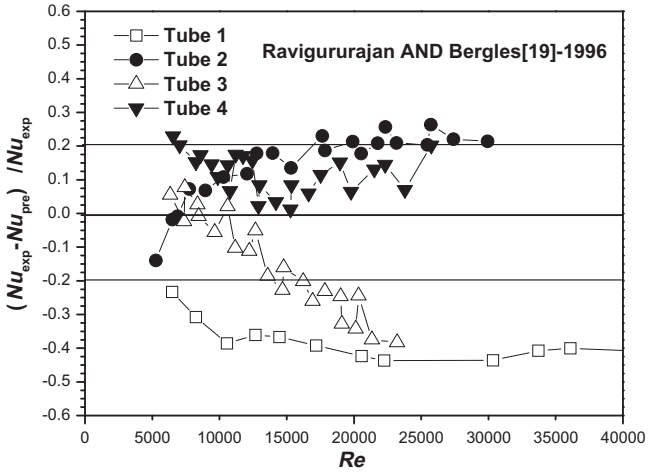

Fig. 12. Comparison of Eq. (5) and experiment results of 4 tubes in [19].

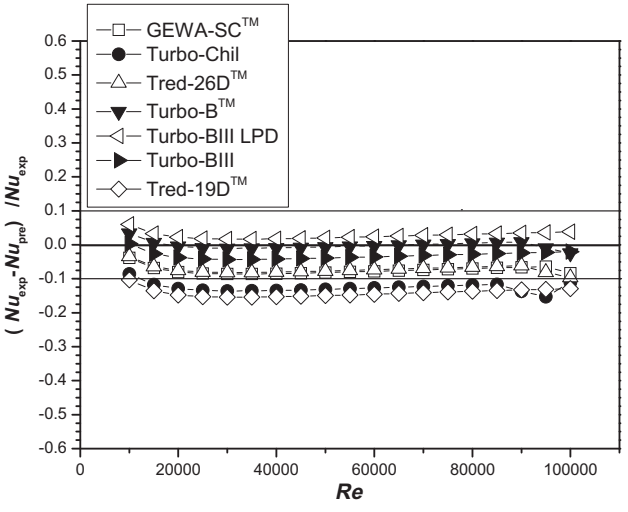

Fig. 11. Comparison of Eq. (8) and Webb's correlation in [20] for the tubes mentioned in the book of Webb and Kim [11].

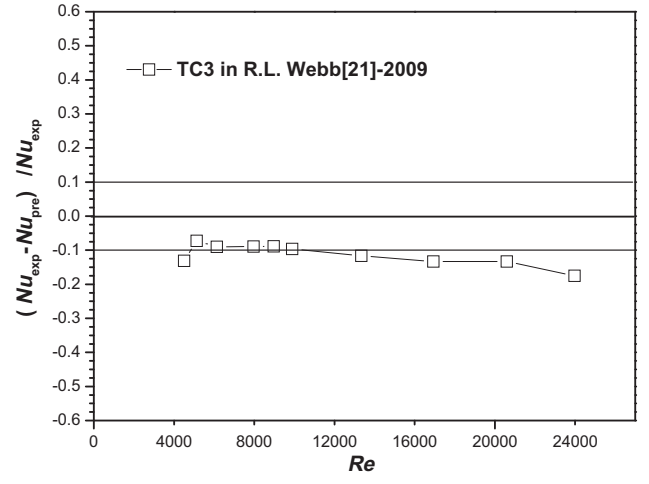

Fig. 13. Comparison of Eq. (8) and experiment results of [21] for the tube of TC3.

Acknowledgment

This work was supported by the National Key Fundamental Research Projects (973) (G2007CB206902, G2011CB710702).

References

[1] V. Gnielinski, New equations for heat and mass transfer in turbulent pipe and channel flows, Int. Chem. Eng. 16 (1976) 359–368.
[2] J.P. Holman, Heat Transfer, eighth ed., McGraw-Hill Book Company (UK) Ltd., Berkshire, England, 1997 (Chapter?).
[3] Y.A. Cengel, Heat Transfer: A Practical Approach, McGraw-Hill, 2003 (Chapter 8).
[4] F.P. Incropera, D.P. DeWitt, T.L. Bergman, A.S. Lavine, Fundamentals of Heat and Mass Transfer, John Wiley & Sons, 2011 (Chapter?).
[5] S.M. Yang, W.Q. TAO, Heat Transfer, fourth ed., Higher Education Press, Beijing, 2006.
[6] G.K. Filonenko, Hydraulic resistance in pipes, Teploenergetika 1 (4) (1954) 40–44.
[7] ER.G. Eckert, R.M. Drake, Heat and Mass Transfer, McGraw-Hill, New York, 1959 (pp. 206).
[8] B.S. Petukhov, V.A. Kurganov, A.I. Gladuntsov, Heat transfer in turbulent pipe flow of gases with variable properties, Heat Transfer-Soviet Res. 5 (4) (1973) 109–116.
[9] B.S. Petukhov, Heat transfer and friction in turbulent pipe flow with variable physical properties, Adv. Heat Transfer 6 (1970) 503–564.
[10] K. Fujie, M. Itoh, T. Innami, H. Kimura, W. Nakayama, T. Yanagida, Heat transfer pipe, U. Patent, No. 4044797, 1977.
[11] R.L. Webb, N.H. Kim, Principle of Enhanced Heat Transfer, second ed., Taylor & Francis, Boca Raton, 2005.
[12] T.B. Styrylska, A.A. Lechowska, Unified Wilson plot method for determining heat transfer correlations for heat exchangers, ASME J. Heat Transfer 125 (4) (2003) 752–756.
[13] E.E. Wilson, A basis for rational design of heat transfer apparatus, Trans. ASME 37 (1915) 47–82.
[14] J.W. Rose, Heat-transfer coefficients Wilson plots and accuracy of thermal measurements, Exp. Therm. Fluid Sci. 28 (2–3) (2004) 77–86.
[15] J. Fernandez-Seara, F.J. Uhia, J. Sieres, A. Campo, A general review of the Wilson plot method and its modifications to determine convection coefficients in heat exchange devices, Appl. Therm. Eng. 27 (17-18) (2007) 2745–2757.
[16] P. Fernando, B. Palm, T. Ameel, P. Lundqvist, E. Granryd, A minichannel aluminium tube heat exchanger - Part I: Evaluation of single-phase heat transfer coefficients by the Wilson plot method, Int. J. Refrig. 31 (4) (2008) 669–680.
[17] F.S. Jose, U. Francisco Jose, S. Jaime, C. Antonio, Experimental apparatus for measuring heat transfer coefficients by the Wilson plot method, Eur. J. Phys. (3) (2005) N1–N11.
[18] H. Shokouhmand, M.R. Salimpour, M.A. Akhavan-Behabadi, Experimental investigation of shell and coiled tube heat exchangers using Wilson plots, Int. Commun. Heat Mass Transfer 35 (1) (2008) 84–92.
[19] T.S. Ravigururajan, A.E. Bergles, Development and verification of general correlations for pressure drop and heat transfer in single-phase turbulent flow in enhanced tubes, Exp. Therm. Fluid Sci. 13 (1) (1996) 55–70.
[20] R.L. Webb, R. Narayanamurthy, P. Thors, Heat transfer and friction characteristics of internal helical-rib roughness, ASME J. Heat Transfer 122 (1) (2000) 134–142.
[21] D. Home, M.F. Lightstone, M.S. Hamed, Validation of DES-SST based turbulence model for a fully developed turbulent channel flow problem, Numer. Heat Transfer Part A: Appl. 55 (4) (2009) 337–361.
[22] M. Strelets, Detached-eddy simulation of massively separated flows, in: Proceedings AIAA Paper 2001-0879, Reno, Nevada, 2001.
[23] M. Assato, M. de Lemos, Turbulent flow in wavy channels simulated with nonlinear models and a new implicit formulation, Numer. Heat Transfer Part A-Appl. 56 (2009) 301–324.
[24] X. Liu, M.K. Jensen, Geometry effects on turbulent flow and heat transfer in internally finned tubes, ASME J. Heat Transfer 123 (6) (2001) 1035–1044.
[25] H.L. Norris Iii, Turbulent Channel Flow with a Moving Wavy Boundary, Stanford University, CA, 1975.
[26] J.H. Kim, K. Jansen, M. Jensen, Analysis of heat transfer characteristics in internally finned tubes, Numer. Heat Transfer Part A: Appl. 46 (1) (2004) 1–21.
[27] R.L. Webb, Single-phase heat transfer, friction, and fouling characteristics of three-dimensional cone roughness in tube flow, Int. J. Heat Mass Transfer 52 (11–12) (2009) 2624–2631.
[28] R.L. Webb, E.R.G. Eckert, R.J. Goldstein, Heat transfer and friction in tubes with repeated-rib roughness, Int. J. Heat Mass Transfer 14 (4) (1971) 601–617.
[30] S.J. Kline, F.A. Mcclintock, Describing uncertainties in single-sample experiments, Mech. Eng. 75 (7) (1953) 3–9.
[31] B. Cheng, W.Q. Tao, Experimental study of R-152a film condensation on single horizontal smooth tube and enhanced tubes, ASME J. Heat Transfer 116 (1) (1994) 266–270.